Proteomics analysis of lung tissue reveals protein makers for the lung injury of adjuvant arthritis rats

PING-HENG ZHANG[1,2], DAN-BIN WU[3], JIAN LIU[4], JIAN-TING WEN[4], EN-SHENG CHEN[1] and CHANG-HONG XIAO[1]

[1]Rheumatology and Immunology Department, Integrated Hospital of Traditional Chinese Medicine, Southern Medical University, Guangzhou, Guangdong 510315; [2]Department of Rheumatology, The First Affiliated Hospital of Guangzhou University of Chinese Medicine, Guangzhou, Guangdong 510405; [3]Department of Traditional Chinese Medicine, School of Medicine, First Affiliated Hospital, Zhejiang University, Hangzhou, Zhejiang 310003; [4]Department of Rheumatology and Immunology, First Affiliated Hospital of Anhui University of Traditional Chinese Medicine, Hefei, Anhui 230038, P.R. China

Received February 13, 2023; Accepted June 15, 2023

DOI: 10.3892/mmr.2023.13051

Abstract. Lung injury is one of the common extra-articular lesions in rheumatoid arthritis (RA). Due to its insidious onset and no obvious clinical symptoms, it can be easily dismissed in the early stage of diagnosis, which is one of the reasons that leads to a decline of the quality of life and subsequent death of patients with RA. However, its pathogenesis is still unclear and there is a lack of effective therapeutic targets. In the present study, tandem mass tag-labeled proteomics was used to research the lung tissue proteins in RA model (adjuvant arthritis, AA) rats that had secondary lung injury. The aim of the present study was to identify the differentially expressed proteins related to RA-lung injury, determine their potential role in the pathogenesis of RA-lung injury and provide potential targets for clinical treatment. Lung tissue samples were collected from AA-lung injury and normal rats. The differentially expressed proteins (DEPs) were identified by tandem mass spectrometry. Bioinformatic analysis was used to assess the biological processes and signaling pathways associated with these DEPs. A total of 310 DEPs were found, of which 244 were upregulated and 66 were downregulated. KEGG anlysis showed that 'fatty acid degradation', 'fatty acid metabolism', 'fatty acid elongation', 'complement and coagulation cascades', 'peroxisome proliferator-activated receptor signaling pathway' and 'hypoxia-inducible factor signaling pathway' were significantly upregulated in the lung tissues of AA-lung injury. Immunofluorescence staining confirmed the increased expression of clusterin, serine protease inhibitors and complement 1qc in lung tissue of rats with AA lung injury. In the present study, the results revealed the significance of certain DEPs (for example, C9, C1qc and Clu) in the occurrence and development of RA-lung injury and provided support through experiments to identify potential biomarkers for the early diagnosis and prevention of RA-lung injury.

Correspondence to: Dr Ping-Heng Zhang or Professor Chang-Hong Xiao, Rheumatology and Immunology Department, Integrated Hospital of Traditional Chinese Medicine, Southern Medical University, 13 Pomegranate Gang Road, Guangzhou, Guangdong 510315, P.R. China
E-mail: 923478117@qq.com
E-mail: xiaochh@smu.edu.cn

Key words: lung injury, adjuvant arthritis, proteomics, tandem mass tag-based quantitation, rheumatoid arthritis

Introduction

Rheumatoid arthritis (RA) is a chronic autoimmune disease characterized by multiarticular synovial inflammation (1), typically leading to progressive, symmetric, erosive polyarthritis (2). It has a high rate of teratogenicity and disability (3). Currently, 0.5-2.0% of the general population is affected by this disease (4). However, RA is not only associated with joint disease but also affects multiple viscera systems. It is well known that due to the abundant connective tissues and blood supply, when the inflammatory factors of the joint synovium entered the blood circulation to reach the lungs, it would cause lung damage, so the lung is frequently affected by RA (5,6). Pulmonary lesion is one of the most common extra-articular lesions in RA, which is an important reason for the decrease in life quality among patients with RA (7). For pulmonary lesions, interstitial lung disease (ILD) is one of the most common RA secondary diseases, accounting for 19-44% of all patients with pulmonary lesions secondary to RA (8). The incidence rate of ILD increases with age (9). Mortality due to secondary ILD accounts for 10-20% of all deaths of patients due to RA and the risk of death is three times higher compared with RA without secondary ILD (10). However, early lung lesions are often asymptomatic and have no radiographic changes, only presenting with lung function decline, and so are easily dismissed by patients (11). As the disease progresses, the patients gradually develop shortness

of breath, exertional dyspnea, restrictive ventilation disorder, reduced diffusion function and hypoxemia, which seriously affect daily life, and eventually lead to pulmonary fibrosis and respiratory failure (12,13). Therefore, pulmonary disease is an important contributor to the decline of quality of life and death in patients with RA (14,15). In this regard, early diagnosis and early prophylactic treatment are essential to prevent the occurrence of interstitial lung disease and reduce the mortality of RA. However, currently, the underlying pathological mechanism is still unclear in RA secondary lung disease, and there is a lack of effective detection means and diagnostic markers for early lung injury in patients with RA (16), and the target of drug therapy is also unclear.

Proteomics, which is a technique that directly quantifies and identifies all proteins in cells and tissues, is currently one of the more comprehensive and effective tools for the identification of drug therapeutic targets and diagnostic markers by the monitoring of changes in protein expression (17). It has been widely used to study the pathogenesis and diagnostic markers of certain rheumatic diseases, including RA (18), ankylosing spondylitis (19) and systemic lupus erythematosus (20). Therefore, proteomics (17) is helpful to investigate the underlying pathogenesis and the key biomarkers in RA lung injury. However, at present, there is a lack of reports about the proteomic analysis of RA lung injury because it is difficult to obtain lung tissue samples in clinical practice (21). In the present study, to improve the diagnosis and better understand the mechanism involved in lung injury in RA at an early stage, a rat model of RA with lung injury was established (22). Finally, an isobaric tandem mass tag (TMT) based quantitative proteomics analysis of the diseased lung tissue and normal lung tissue was performed in the rat model. The results of this study may give new insight into the molecular basis of the pathogenesis of RA lung injury, and provide new clues for the early diagnosis and prevention of RA lung injury.

Materials and methods

Animals and experimental design. Twelve male 6-week-old Sprague-Dawley (SD) rats (weight, 180-200 g) were provided by Anhui Laboratory Animal Center [animal License number: scxk (Anhui) 2011-002]. The present study was approved by the Animal Ethics Committee of Anhui University of Traditional Chinese Medicine (approval no. AHUCM-RATS-2021022) and complied with the guide for the Health Care and Use of Laboratory Animals (23). The rats were placed in the clean-grade experimental animal room for adaptive feeding for a week, maintained under a 12-h dark/light cycle and provided with food and water *ad libitum*, while the room environment was kept quiet. The temperature was maintained at 16-25˚C and humidity at 50-75%. The 12 SD rats were randomly divided into two groups, including control (CN, n=6) and AA (n=6) groups. Except for the CN group, the other rats were injected with 0.1 ml Freund's complete adjuvant (FCA; MilliporeSigma) in the right rear paw to establish the AA model at 7 weeks old. On the 7th day after modeling, 5 mg/ml Bacillus Calmette-Guerin (Guangzhou Yi Yi Neng Biotechnology Co., Ltd.) 0.05 ml was injected into the tail root of AA model rats to enhance immunization. After 4 weeks, the AA lung injury model was considered to be established (22). The lung function of the rats, which included forced vital capacity (FVC), forced expiratory volume at 0.2 sec (FEV0.2), FEV 0.2 sec/FVC, peak expiratory flow (PEF) and expiratory flow 50% (FEF50) was assessed using an animal lung function apparatus (Ani Res 2003) (24). Subsequently, all rats were sacrificed by cervical dislocation after anesthesia with 50 mg/kg pentobarbital sodium by intraperitoneal injection after testing the lung function of the rats before the experimental endpoint, and lung tissue was collected. Part of the lung tissues in each rat was taken and washed with 0.9% sodium chloride solution and immediately immersed in liquid nitrogen for subsequent experiments. The remaining lung tissues were used for H&E, Masson staining and western blotting.

Joint swelling and arthritis score. Joint swelling and arthritis score were assessed every 7 days after model establishment for 4 weeks. The criteria for arthritis score (25) were as follows: i) Normal, 0 points; ii) ankle/wrist joint swelling, 1 point; iii) swelling of ankle or wrist, 2 points; iv) severe swelling of the whole claw, 3 points; v) foot deformity or stiffness, 4 points. The joint swelling of AA rats was detected by a paw volume measuring instrument (cat. no. PV-200; Chengdu Taimeng Co., Ltd.).

Hematoxylin and eosin (H&E) and Masson staining of lung tissue. For histological examination, part of the rat fresh lung tissue was taken and rapidly fixed in a 4% formaldehyde solution for 48 h at room temperature, followed by dehydration (slides washed in 100, 95, 80 and 75% alcohol for 2 min each), embedding and sectioning (4 μm). Finally, the paraffin blocks were stained with H&E for 5 min at room temperature or Masson staining (cat. no. G1340; Beijing Solarbio Science & Technology Co., Ltd.) (26) for 3 min at room temperature following the manufacturer's instructions. A Leica DMIL light microscope was used to image the sections. The Szapiel method (27) was used to assess the extent of alveolar inflammation, and the results were expressed with scores of alveolitis. Fibrosis tissue was quantified using Image Pro Plus 6.0 (Media Cybernetics Corporation). Results were presented as the percentage of the total area of the field of view (five fields of view in each group), which was occupied by fibrosis.

TMT-labeled quantitative proteomics. A total of 100 mg frozen lung tissue was added to the 1 ml SDT (4% SDS, 100 mM Tris-HCl, 1 mM dithiothreitol, pH 7.6) lysis buffer. The lung tissue was subsequently homogenized using an MP homogenizer and crushed with an ultrasonic crusher in the ice bath. The homogenized lysate was then further processed in a boiling water (100˚C) bath for 10 min. After centrifugation at 14,000 x g for 15 min at 4˚C, the supernatant was filtered using a 0.22-μm centrifugal tube, and the filtrate was collected. The protein concentration of the samples was determined using a BCA protein assay kit (Bio-Rad Laboratories, Inc.). A total of 200 μg protein lysate was collected from each sample and trypsinized by the filter aided sample preparation method (28). The peptides were desalted using a C18 column (Thermo Fisher Scientific, Inc.; Acclaim PepMap RSLC 50 μm x 15 cm; nano viper; P/N164943). After freeze-drying, the peptide segments were redissolved by adding 40 μl of 0.1% formic acid solution. TMTsixplex™ labeling reagent set (cat. no. 90064CH;

Thermo Fisher Scientific, Inc.) was used for labeling. High pH reversed peptide separation kit (cat. no. 84868; Thermo Fisher Scientific, Inc.) was used for grading. Consequently, to introduce more sample information about the AA group, the six samples were combined to form three different samples. The same procedure was used for the control group.

Liquid chromatography-tandem mass spectrometry (LC-MS/MS) analysis was performed using Easy-nLC with nanoflow high-performance liquid chromatography liquid phase system (Thermo Fisher Scientific, Inc.). A total of 1 μg of each sample was loaded into a chromatographic column and separated by an analytical column with a 300 nl/min flow rate, an ion spray voltage of 2.0 kV and an ion transfer tube temperature of 320˚C. Samples were then run through to a Q-Exactive Orbitrap Mass Spectrometer (Thermo Fisher Scientific, Inc.) for 90 min. The mass spectrometer was used in the positive ion mode. MS spectra were acquired over a range of 300-1,800 m/z, using a data-dependent collection method, which dynamically selected the most abundant precursor ions from measurement scans (range 300-1,800 m/z). MS scan was acquired at a resolution of 70,000 at 200 m/z and 15,000 at 100 m/z for MS/MS scan. The isolation window was 2 m/z and the normalized collision energy was 30 eV. The maximum ion implantation time for the measurement scan was set to 50 msec, the MS/MS scan was set to 100 msec, the automatic gain control target values for the full scan mode were set to $1x10^6$, and was set to $5x10^4$ for MS/MS. The dynamic exclusion time was 60 sec. A schematic representation of the experimental procedure of TMT-labeled quantitative proteomics is presented in Fig. 1.

Bioinformatics analysis. To improve the study of the biological functions of differential proteins, bioinformatics analysis was performed. Compared with those in the CN group, proteins with P-value <0.05 and fold-change >1.20 (upregulated >1.20 times or downregulated <0.83 times) were considered to be differentially regulated proteins in the AA group, and the volcano plot and heatmap plot were visualized by tbtools (29). The analysis of the differentially regulated proteins was performed using Mascot 2.2 (Matrix Science, Inc.) and Proteome Discoverer 1.4 software (Thermo Fisher Scientific, Inc.). The Gene Ontology (GO) and Kyoto Encyclopedia of Genes and Genomes (KEGG) databases with default parameters were used to perform functional annotation and biological pathway analysis of the identified proteins by clusterProfiler, the P-value of <0.05 was considered as significant enrichment, and the visualization performed with bubble plot and cnet plot. The protein-protein interactions (PPIs) were used to construct the interaction model between different proteins. The Search Tool for the Retrieval of Interacting Genes/Proteins (STRING) database (https://cn.string-db.org/; version 11.5) was used to visualize the interaction relationship between different proteins and to predict the mechanism of action.

Immunofluorescence. The fresh lung tissues of rats were fixed in 4% paraformaldehyde solution for 48 h at room temperature and then paraffin embedded and sliced at room temperature. The lung tissues were sectioned in a microtome with a thickness of ~8 μm. The lung tissue sections were then heated in a 60˚C incubator for 45 min to dewax the slices, which were then immersed in xylene I for 10 min, xylene II for 10 min, absolute ethanol I (100% ethanol) for 5 min, absolute ethanol II (100% ethanol) for 5 min, 95% ethanol for 3 min, 80% ethanol for 3 min, 70% ethanol for 3 min and rinsed with PBS for 5 min, all at room temperature. The lung tissue sections were then treated with boiling (100˚C) citric acid (pH 6.0) for antigen retrieval for 20 min. After cooling naturally at room temperature, the sections were washed with PBS 3 times (5 min each) The lung tissue sections were then treated with 0.5% Triton for 4.5 min and washed with PBS 3 times (5 min each). The sections were then blocked using 5% BSA (Beijing Solarbio Science and Technology Co., Ltd.) for 20 min at room temperature. The sections were incubated with primary antibodies against C1qc (1:100; cat. no. A05666; Boster Biological Technology), C9 (1:100; cat. no. K107807P; Beijing Solarbio Science and Technology Co., Ltd.), Clu (1:100; cat. no. 12289-1-AP; Proteintech Group, Inc.) at 4˚C overnight and washed with PBS 3 times (5 min each). The sections were then incubated with FITC (1:500; cat. no. A0562; Beyotime Institute of Biotechnology) or Cy3 (1:500; cat. no. A0516; Beyotime Institute of Biotechnology)-labeled goat anti-rabbit IgG (H+L) secondary antibodies for 20 min at room temperature. The sections were counter stained using 1 μg/ml DAPI for nuclear staining for 15 min at room temperature, washed with PBS 3 times (5 min each) and sealed using an anti-fluorescence quenched tablet (cat. no. S2100; Beijing Solarbio Science & Technology Co., Ltd.). A Leica DM14000B laser confocal microscope was used to image the samples and 5 fields of view were randomly selected for each lung tissue section (magnification, x400); The immunofluorescence micrographs were analyzed quantitatively with the fraction of positive area in each image analyzed using ImageJ software ij149 (National Institutes of Health).

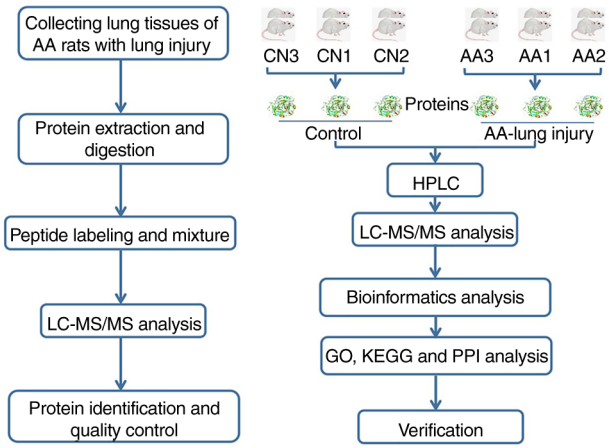

Figure 1. Schematic representation of the experimental process in the present study. Lung tissue samples from six normal Sprague-Dawley rats and six AA rats were included in the present study. The lung injury of AA rats was assessed according to changes in lung function and histology. Proteins extracted from the lung tissues were labeled with tandem mass tag and subsequently subjected to LC-MS/MS analysis. Bioinformatics analysis of differential protein expression function was verified by immunofluorescence analysis. AA, adjuvant arthritis; LC-MS/MS, liquid chromatography-tandem mass spectrometry; CN, control; HPLC, high-performance liquid chromatography.

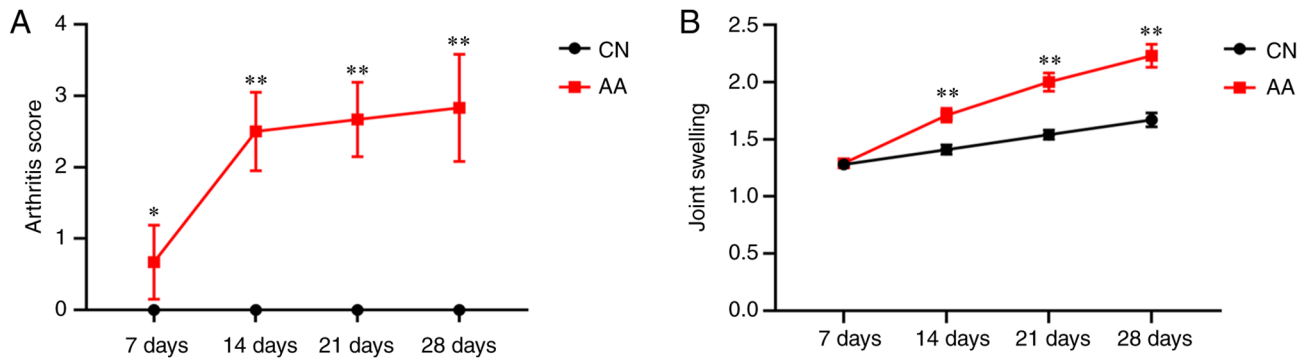

Figure 2. Arthritis score and joint swelling in AA rats. After the rats were injected with Freudian complete adjuvant, (A) arthritis score and (B) joint swelling were evaluated on days 7, 14, 21 and 28. *P<0.05 or **P<0.01 vs. CN group in rats. CN, control; AA, adjuvant arthritis; d, day.

Statistical analysis. SPSS software (version 22.0; IBM Corp.) was used to perform statistical analysis. Standard deviation was used to evaluate the dispersion of the data. An independent unpaired Student's t-test was used to evaluate the results and the Pearson correlation test was used for the analysis of continuous variables. Wilcoxon test was employed to compare the different proteins between the AA and CN groups. Results are expressed as the mean ± standard deviation. P<0.05 was considered to indicate a statistically significant difference.

Results

Examination of arthritis score and joint swelling. To evaluate the success of the AA model, arthritis score and joint swelling were assessed every 7 days starting from the 7th day after modeling and continuing for a total of 4 weeks. After modeling, the joint swelling and arthritis scores were demonstrated to be significantly increased in the AA group compared with those in the CN group. Therefore, the results indicated that the AA model was successfully established in the present study (Fig. 2A and B).

Effects of lung injury in AA rats. A previous study showed that inflammatory infiltration of the lungs begins 21 days after modeling, whilst pulmonary fibrosis and pleural thickening begins after 28 days (22). Therefore, lung tissues of AA rats were collected 4 weeks after modeling in the present study. To identify lung injury in AA, the lung function in AA rats was assessed by using an animal lung function instrument and evaluation of the histopathology of lung tissues by using H&E and Masson staining. The present study evaluated the lung function, the inflammatory degree and the collagen deposition of lung tissue 4 weeks after modeling in AA. Swollen, diminished and damaged structures were observed in the pulmonary alveoli of the AA group compared with those in the CN group (Fig. 3A). Besides, severe inflammatory infiltration was found in the lung interstitium (Fig. 3A). Meanwhile, thickened alveolar walls, widened alveolar septa and the deposition of collagen fibrin (blue deposits in Fig. 3B) were also observed. The scores of alveolitis and the area of fibrosis were significantly increased in the AA group compared with those in the CN group (Fig. 3C and D), whilst the lung function indexes (including FVC, $FEV_{0.2}$, $FEV_{0.2}$/FVC, PEF and FEF_{50}) were significantly decreased in the AA group compared with those in the CN group) (Fig. 3E).

In the present study, a correlation analysis between the joint swelling and arthritis score and pulmonary function and fibrosis area of AA rats was performed. This demonstrated that joint swelling was significantly positively correlated with fibrosis area and significantly negatively correlated with FVC. Furthermore, the arthritis score was significantly negatively correlated with $FEV_{0.2}$ and $FEV_{0.2}$/FVC (Table SI).

Identification of DEPs in the lung tissue of AA rats. In the present study, the effect of RA on lung tissue was investigated. TMT-labeled proteomics was used to evaluate the changes in the expression of all proteins in the lung tissue of AA rats compared with those in CN rats. A total of 6,693 proteins or unique peptides were identified in AA rat lung tissue (Fig. 4A and B). Through the screening of DEPs, 244 upregulated proteins and 66 downregulated proteins were identified in the lung tissue of AA rats according to the criteria described in the methods, fold change >1.20 (upregulated >1.20 times or downregulated <0.83 times compared with CN rats) and P<0.05. The top 20 DEPs that were upregulated and downregulated are listed in Tables I and II, respectively. The majority of the top 20 DEPs were related to fatty acid metabolism, immunity, lung inflammation, fibrosis and cancer (Tables I and II).

GO analysis of DEPs. To better assess the function of DEPs in the lung tissue of the AA group, their activity, localization and function in biological processes, cellular components and molecular functions were assessed using GO enrichment analysis with cluster profile. The results of enrichment analysis identified 3,764 biological processes (BPs), 418 cellular components (CCs) and 572 molecular functions (MFs); of which 983 terms were significantly enriched, including 741 BPs, 90 CCs and 152 MFs (data not shown). The top 10 enriched BP terms included 'complement activation, classical pathway' (GO:0006958), 'generation of precursor metabolites and energy' (GO:0006091), 'humoral immune response mediated by circulating immunoglobulin' (GO:0002455), 'response to endoplasmic reticulum (ER) stress' (GO:0034976), 'cellular response to reactive oxygen species' (GO:0034614), 'complement activation' (GO:0006956), 'protein folding' (GO:0006457), 'response to reactive oxygen species'

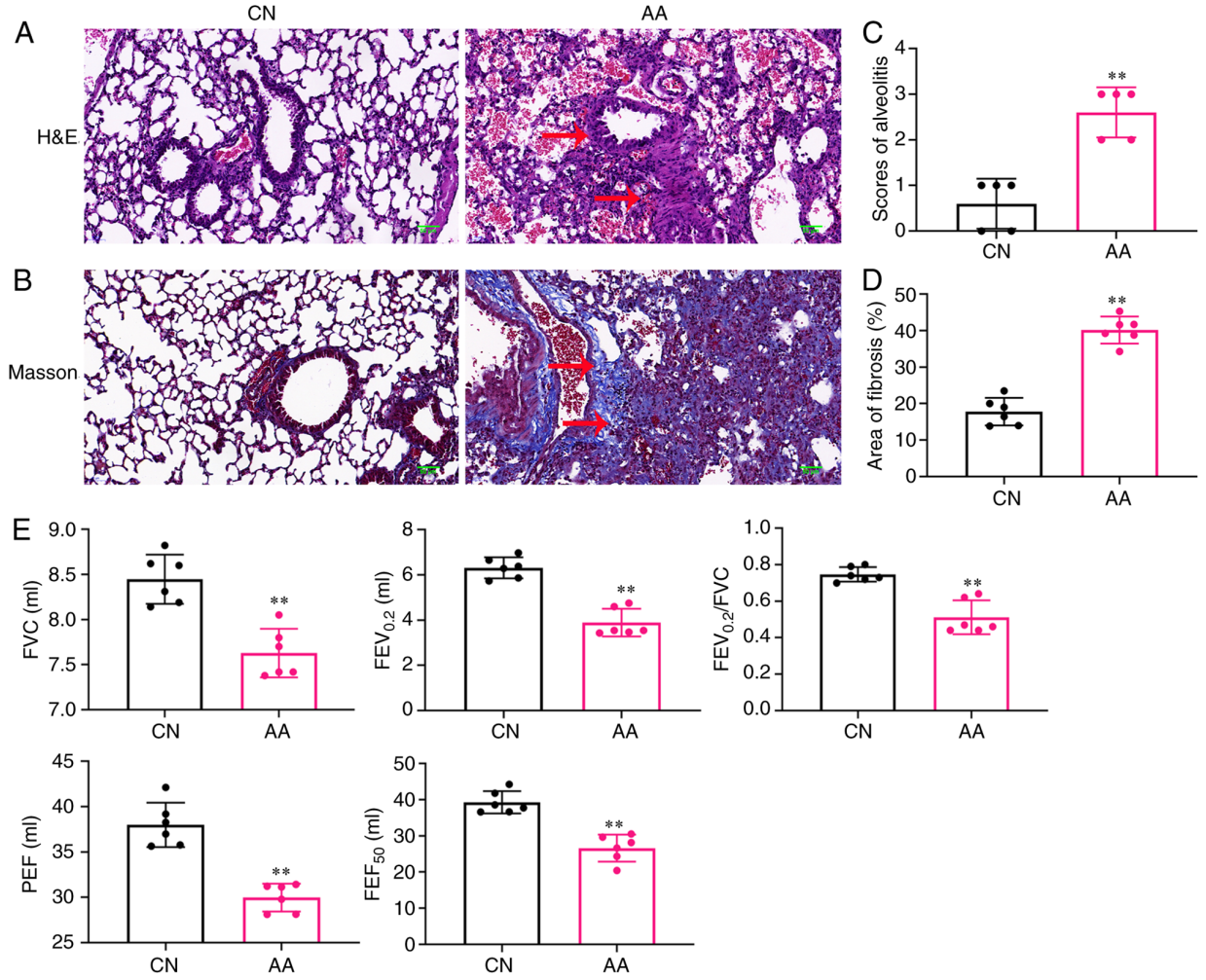

Figure 3. Histopathology of lung tissues was assessed in AA rats. (A) H&E staining of lung tissues in AA rats (x400 magnification). (B) Masson staining of lung tissues in AA rats (Masson x400). (C) Scores of alveolitis of lung tissues in AA rats. (D) The area of fibrosis in AA rats. (E) The lung function in AA rats. **P<0.01 vs. CN group in rats. CN, control; AA, adjuvant arthritis; H&E, hematoxylin and eosin; FVC, forced vital capacity; $FEV_{0.2}$, forced expiratory volume at 0.2 sec; PEF, peak expiratory flow; FEF_{50}, expiratory flow 50%.

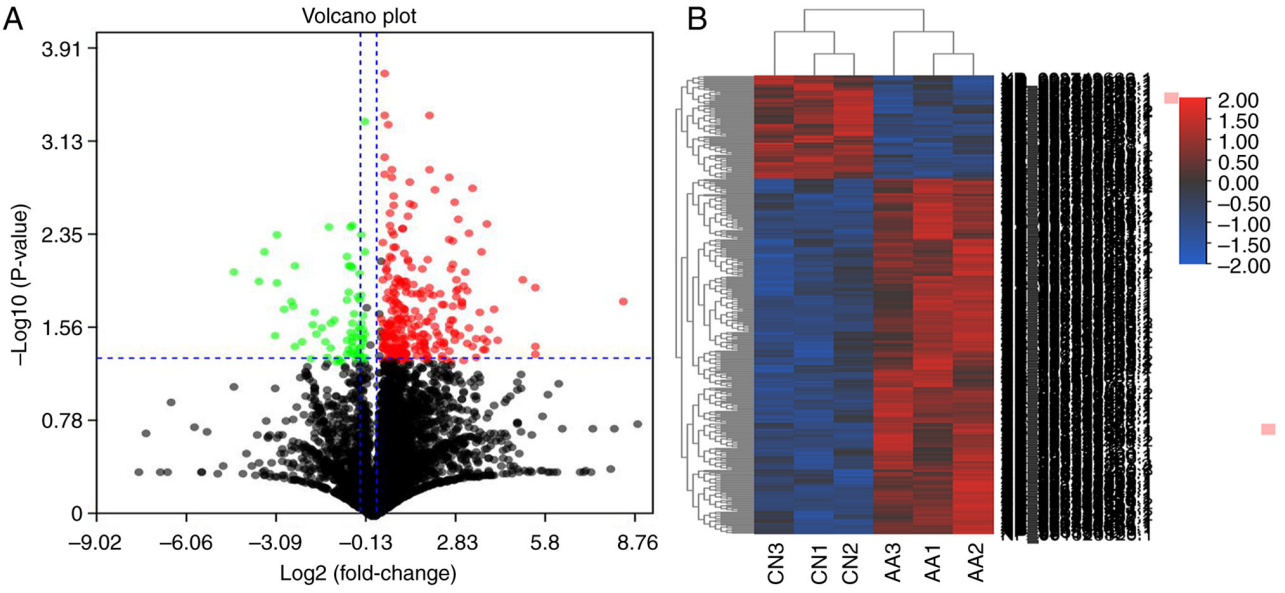

Figure 4. Proteomic analysis of lung injury of AA rats. (A) Volcano plot of DEPs in AA group vs. CN group. Green dots represented downregulated proteins, red dots represent upregulated proteins, and black dots showed proteins with no statistically significant difference between AA group vs. CN group. (B) Heatmap of 310 DEPs between AA group and CN group. Red represented upregulation and blue represented downregulation of expression when compared with CN group. CN, control; AA, adjuvant arthritis; DEPs, differentially expressed proteins.

Table I. Top 20 upregulated differentially expressed proteins in lung tissue of adjuvant arthritis rats.

Protein ID	Symbol	Name	Fold change	P-value
NP_001020037.1	CFAP36	Cilia and flagella associated protein 36	41.672	$3.77x10^{-2}$
NP_058830.2	ARG1	Arginase 1	40.085	$4.39x10^{-2}$
NP_037073.1	CYP51A1	Cytochrome P450 51A1	17.412	$3.31x10^{-2}$
XP_006233064.1	HMGCS2	3-hydroxy-3-methylglutaryl-coa synthase 2	15.824	$1.81x10^{-2}$
NP_001013068.1	POLD2	DNA polymerase delta 2, accessory subunit	13.794	$2.65x10^{-2}$
NP_036769.1	PTPN1	Protein tyrosine phosphatase, non-receptor type 1	13.718	$3.45x10^{-3}$
NP_059049.1	SLC7A5	Solute carrier family 7 member 5	13.709	$3.37x10^{-2}$
NP_445739.1	B4GALT1	B-1,4-galactosyltransferase 1	12.978	$4.01x10^{-2}$
NP_001099511.1	CTSG	Cathepsin G	12.553	$3.24x10^{-2}$
NP_387500.1	MCM4	Minichromosome maintenance complex component 4	12.210	$3.91x10^{-2}$
NP_037245.2	ATP1B1	Atpase Na+/K+ transporting subunit β 1	11.377	$1.93x10^{-2}$
XP_006256782.1	WDR13	WD repeat domain 13	10.644	$4.68x10^{-2}$
XP_003750198.1	PNPLA8	Patatin-like phospholipase domain containing 8	10.549	$3.26x10^{-2}$
NP_001008889.1	YOD1	YOD1 deubiquitinase	9.687	$1.73x10^{-3}$
NP_001014020.2	PDE12	Phosphodiesterase 12	9.038	$4.23x10^{-3}$
NP_001019435.1	PRTN3	Proteinase 3	8.963	$2.60x10^{-2}$
NP_001100237.1	ELANE	Elastase, neutrophil expressed	8.598	$1.27x10^{-2}$
NP_001012103.1	TRIM32	Tripartite motif-containing 32	8.556	$3.49x10^{-2}$
NP_062243.2	ENPP3	Ectonucleotide pyrophosphatase/ phosphodiesterase 3	8.259	$8.76x10^{-3}$
NP_001008721.1	EBNA1BP2	EBNA1 binding protein 2	7.873	$4.94x10^{-2}$

Table II. Top 20 downregulated differentially expressed proteins in lung tissue of adjuvant arthritis rats.

Protein ID	Symbol	Name	Fold change	P-value
XP_006244031.1	CMTM6	CKLF-like MARVEL transmembrane domain containing 6	0.073	$1.06x10^{-2}$
NP_001102028.1	THEM5	Thioesterase superfamily member 5	0.083	$6.07x10^{-3}$
NP_001166922.1	VPS25	Vacuolar protein sorting 25 homolog	0.111	$4.27x10^{-3}$
NP_620260.2	PLPP3	Phospholipid phosphatase 3	0.163	$7.76x10^{-3}$
NP_001099769.1	AHSP	A hemoglobin stabilizing protein	0.167	$3.76x10^{-2}$
NP_001138331.2	KIAA0408L	Kiaa0408-like	0.195	$3.42x10^{-2}$
NP_001100706.1	COBL	Cordon-bleu WH2 repeat protein	0.247	$2.42x10^{-2}$
XP_006241073.1	POLR2E	RNA polymerase II, I and III subunit E	0.308	$2.65x10^{-2}$
NP_001178629.1	OTUD4	OTU deubiquitinase 4	0.348	$4.64x10^{-2}$
NP_001102459.1	KANK3	KN motif and ankyrin repeat domains 3	0.383	$2.38x10^{-2}$
NP_942058.1	SLC1A4	Solute carrier family 1 member 4	0.384	$3.81x10^{-2}$
NP_446253.2	SEC14L2	SEC14-like lipid binding 2	0.410	$2.26x10^{-2}$
NP_001010968.1	ENG	Endoglin	0.426	$4.98x10^{-2}$
XP_006243178.1	PEAK1	Pseudopodium-enriched atypical kinase 1	0.436	$4.73x10^{-2}$
NP_001009663.1	SERPINA6	Serpin family A member 6	0.469	$4.90x10^{-2}$
NP_001009639.1	TPPP3	Tubulin polymerization-promoting protein family member 3	0.540	$3.37x10^{-2}$
NP_001020859.1	PALMD	Palmdelphin	0.544	$4.33x10^{-2}$
NP_001008562.1	LMCD1	LIM and cysteine-rich domains 1	0.548	$6.60x10^{-2}$
NP_001013185.1	WASF2	WASP family member 2	0.566	$3.99x10^{-2}$
NP_062026.2	FBLN5	Fibulin 5	0.570	$1.32x10^{-2}$

(GO:0000302), 'fatty acid metabolic process' (GO:0006631) and 'cholesterol biosynthetic process' (GO:0006695). The top 10 enriched CC terms were 'membrane region' (GO:0098589), 'mitochondrial matrix' (GO:0005759), 'membrane raft' (GO:0045121), 'membrane microdomain' (GO:0098857), 'ER chaperone complex' (GO:0034663),'ER lumen' (GO:0005788), 'smooth ER' (GO:0005790), 'minichromosome maintenance protein (MCM) complex' (GO:0042555), 'plasma membrane raft' (GO:0044853) and 'focal adhesion' (GO:0005925). The top 10 enriched MF terms were 'NAD binding' (GO:0051287), 'ribonucleoprotein complex binding' (GO:0043021), 'chaperone binding' (GO:0051087), 'misfolded protein binding' (GO:0051787), 'amide binding' (GO:0033218), 'ribosome binding' (GO:0043022), 'integrin binding' (GO:0005178), 'sulfur compound binding' (GO:1901681), 'oxidoreductase activity, acting on the CH-CH group of donors' (GO:0016627) and 'complement binding' (GO:0001848). The top 10 BP, CC and MF terms related to DEPs, according to enrichment factor with the genes related to these terms were presented in a in cnet plot (Fig. 5A-C).

In summation, the results of the present study suggested that RA may be related to the dysregulation of the biological process of the metabolic process, such as the metabolic process of fatty acid, cholesterol, secondary alcohol and steroid, response to stimulus, such as response to ER stress, cellular response to reactive oxygen species, and immune and inflammatory response, such as complement activation, immune response to immunoglobulin. According to the bioinformatic analysis RA affected proteins serving numerous roles, which were closely involved in cell damage.

KEGG pathway and DEPs. To further analyze the biological processes, a cluster profile was employed for KEGG pathway analysis of DEPs in lung tissues from the AA group compared with the CN group. This analysis enabled the identification of the most important signal transduction pathways and biochemical metabolic pathways that were related to the genes encoding DEPs. The top 25 enrichment KEGG pathway terms are shown in Fig. 6A. The results suggested that the majority of DEPs were associated with 'fatty acid degradation', 'fatty acid metabolism', 'fatty acid elongation', 'complement and coagulation cascades', 'peroxisome proliferator-activated receptor (PPAR) signaling pathway' and 'hypoxia-inducible factor (HIF)-1 signaling pathway' (Fig. 6A). The upregulated DEPs related to fatty acids metabolic processes included ER lipid raft protein (ERLIN) 1, thioesterase superfamily protein, acyl-CoA dehydrogenase long chain (ACADL), acyl-CoA dehydrogenase medium chain (ACADM) and acyl-CoA oxidase 1 (ACOX1). The upregulated DEPs associated with complement and coagulation cascades included complement (C)-9, C4a, C1qc, Cfb, clusterin (Clu), C4 binding protein a (C4bpa) and serine protease inhibitors (SERPING) 1. The upregulated DEPs associated with the PPAR signaling pathway included glucokinase, fatty acid-binding protein 5, 3-hydroxy-3-methylglutaryl-coenzyme A synthase 2 (mitochondrial), ACADL, recombinant carnitine palmitoyltransferase 2 and ACOX1. The upregulated DEPs associated with the HIF-1 signaling pathway, included pyruvate dehydrogenase (lipoamide) α 1, cytochrome b-245 β chain, cullin 2 polypeptide, mitogen activated protein kinase 3 (MAPK3), transferrin receptor, hexokinase (HK) 3, HK2 and GAPDH. In the pathway enrichment analysis, each KEGG pathway was used as a unit to correlate pathways that were significantly enriched by DEPs. The present study determined the most important signal transduction pathways and biochemical metabolic pathways of DEPs in the lung tissue of AA-lung injury rats through pathway enrichment analysis (Fig. 6B). The majority of the proteins enriched KEGG pathway in the top 25 terms were related to lung injury and immunity, which were located in the 'fatty acid degradation', 'fatty acid metabolism', 'fatty acid elongation', 'complement and coagulation cascades', 'peroxisome proliferator-activated receptor (PPAR) signaling pathway' and 'hypoxia-inducible factor (HIF)-1 signaling pathway'.

PPI network analysis of DEPs. To elucidate the interaction between the DEPs, PPI analysis was performed on the 307 DEPs in the STRING database. The PPI network generated, consisted of 273 DEPs and 2,218 pairs of interactions (Fig. 7). The connectivity degree was high for dozens of gene nodes, such as glutamyl-prolyl-tRNA synthetase (fold change=1.448, $P=6.50x10^{-3}$), heat shock protein family A (Hsp70) member 5 (fold change=1.313, $P=1.88x10^{-4}$), GAPDH (fold change=1.295, $P=4.31x10^{-4}$), eukaryotic translation elongation factor 2 (fold change=1.398, $P=2.49x10^{-2}$), Tu translation elongation factor, mitochondrial (fold change=1.425, $P=9.82x10^{-3}$), integrin subunit β 2 (ITGB2, fold change=2.749, $P=1.34x10^{-2}$), protein tyrosine phosphatase receptor type C (fold change=2.157, $P=4.30x10^{-2}$), eukaryotic translation elongation factor 1 γ (fold change=1.355, $P=3.94x10^{-2}$), Hsp70 member 9 (fold change=1.622, $P=4.37x10^{-3}$), ACADM (fold change=1.353, $P=3.16x10^{-2}$), MAPK3 (fold change=0.729, $P=4.73x10^{-2}$) and integrin subunit β1 (fold change=0.759, $P=3.77x10^{-2}$). The details of the top 10 down-and upregulated genes with the highest degree of connectivity are provided in Table III.

Validation of DEPs. Among the DEPs, C1qc, C9 and Clu, which were the upregulated proteins associated with complement and coagulation cascades by employing KEGG pathway analysis, were selected for validation in the lung tissues of rats by immunofluorescence. The immunofluorescence results demonstrated that the protein expression levels of C1qc, C9 and Clu were significantly increased in AA rats compared with the CN rats (Fig. 8). These results were consistent with the results of the aforementioned proteomic analysis.

Discussion

Lung injury is an important form of extra-articular lesions in RA, which is an important cause for the decline of the quality of life, and death, in patients with RA (30). Currently, the pathogenesis of lung injury in RA remains unclear. Clinically, there is a lack of biomarkers that can be used for the early diagnosis of RA lung injury. Given the difficulty in obtaining lung tissue from patients with RA, previous studies (31,32) have reported the relevance of using AA animal models (mature RA animal models), which have lung injuries such as decreased lung function and ILD, which can be produced by using FCA-induce AA. Therefore, an AA rat model was used as an alternative *in vivo* model in the present study. The results of the present study indicated that the rats demonstrated obvious joint swelling and significantly increased arthritis

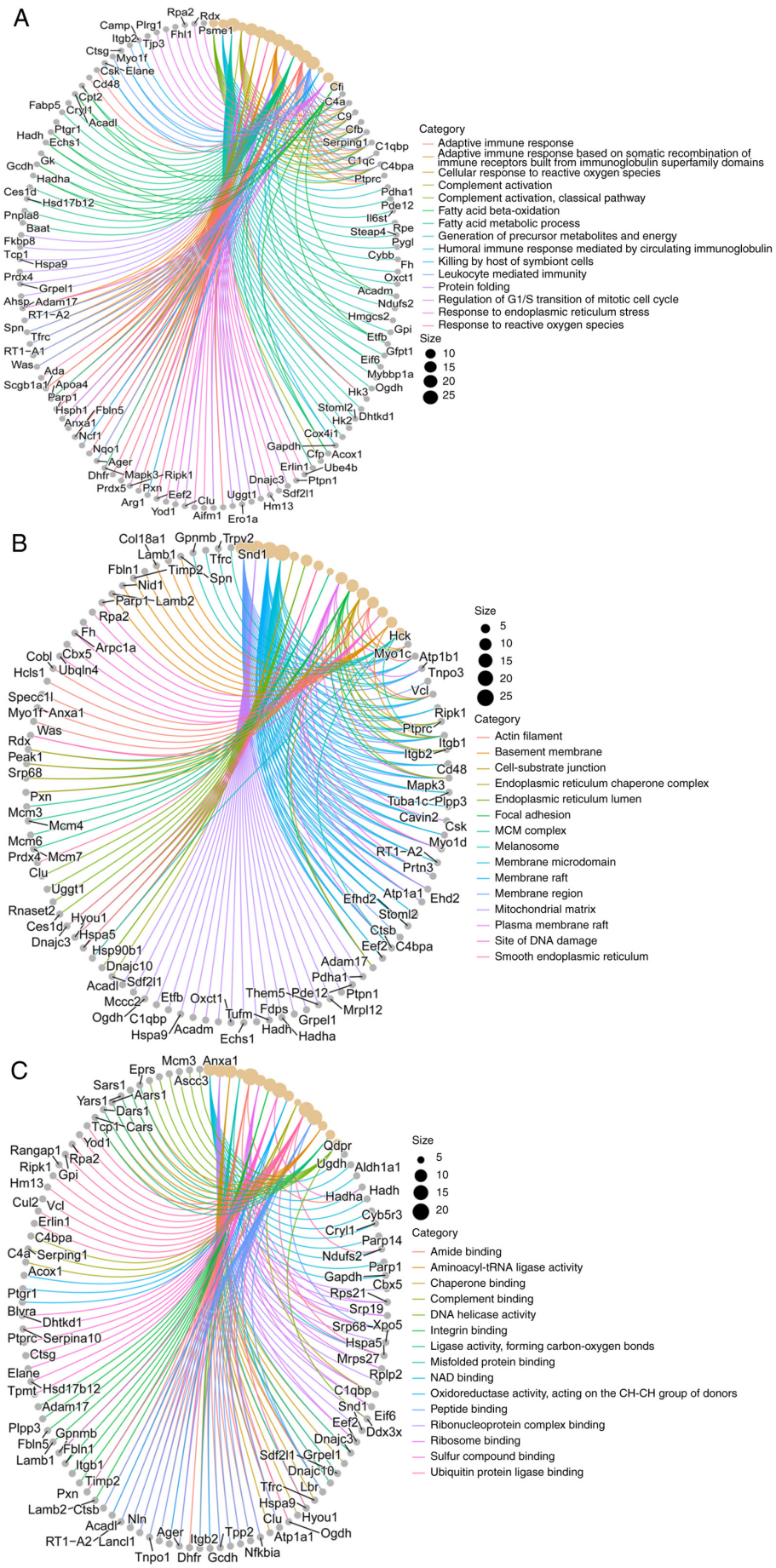

Figure 5. Gene ontology analysis of proteins differentially expressed between adjuvant arthritis-lung injury and control mice. (A) Biological Processes. (B) Cellular Components. (C) Molecular Functions. The term 'size' indicates the number of genes.

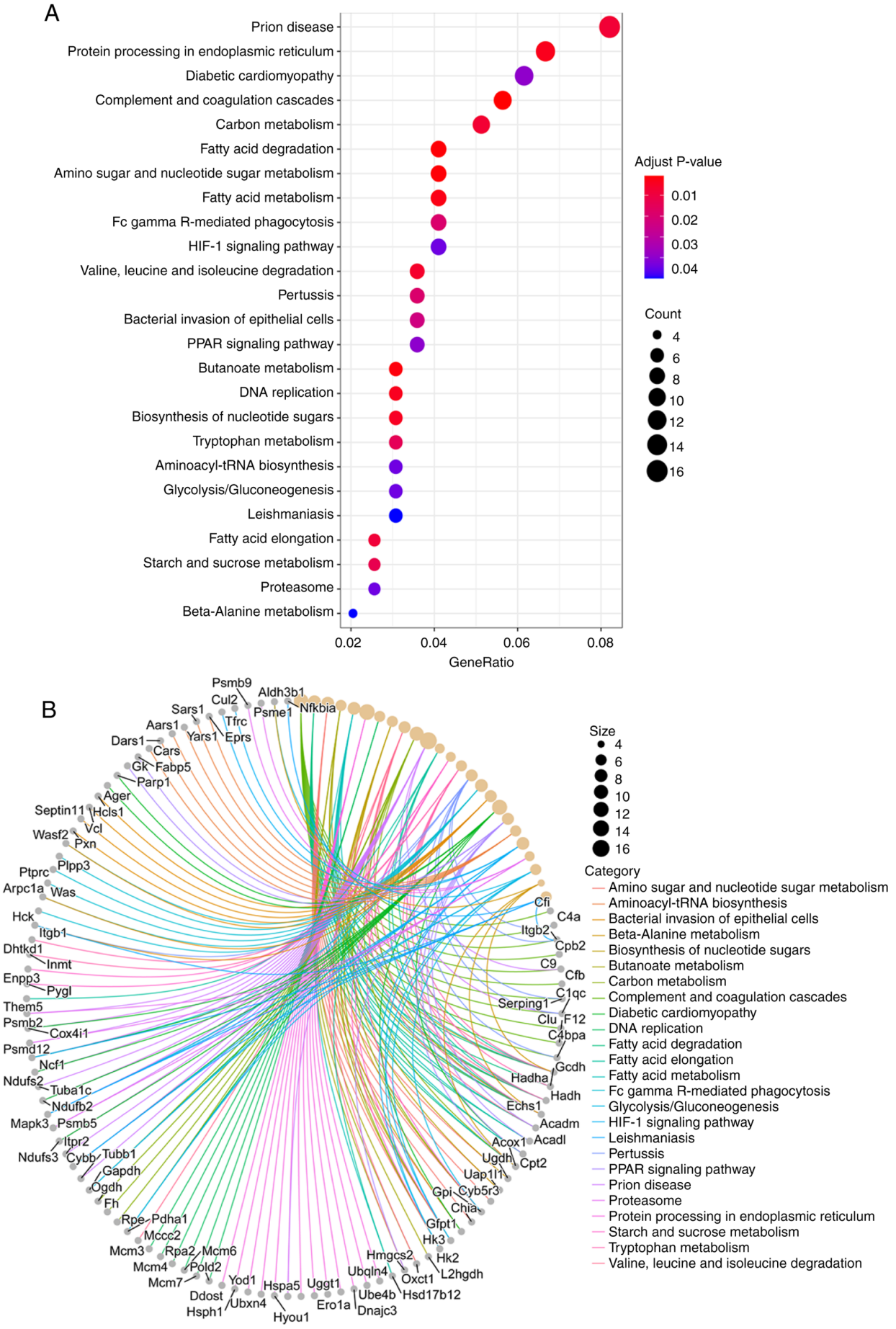

Figure 6. KEGG pathway annotation and enrichment. (A) Top 25 pathway of KEGG pathway annotation. (B) Differentially expressed genes on each pathway of KEGG enrichment. The term 'size' indicates the number of genes. KEGG, Kyoto Encyclopedia of Genes and Genomes.

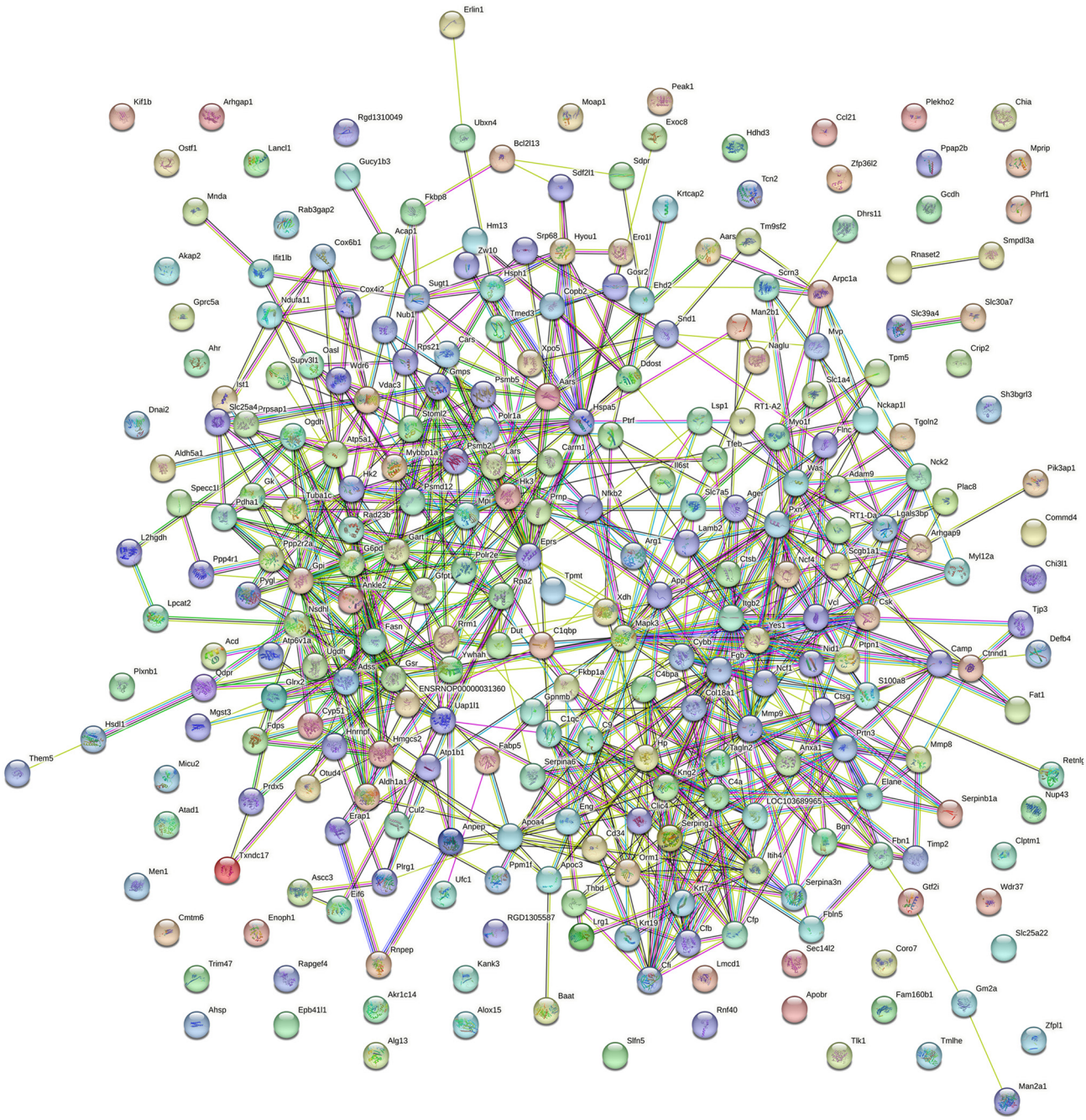

Figure 7. PPI network analysis of DEPs. A critical assessment and integration of PPIs with DEPs by STRING, including direct (physical) as well as indirect (functional) associations. PPI, protein-protein interaction; DEPs, differentially expressed proteins.

scores on day 7 after injection with FCA, which indicated the successful establishment of the AA model. On the day 28 after modeling with FCA and BCG, swollen, diminished and damaged structures were observed in pulmonary alveoli in the AA group compared with those in the CN. Furthermore, severe inflammatory infiltration (as determined by HE staining and score of alveolitis) was found in the lung interstitium. Meanwhile, thickened alveolar walls, widened alveolar septa and the deposition of collagen fibrin were also observed. This was consistent with the results reported by Song *et al* (22). These results further validated the model of AA lung injury used in the present study. Subsequently, proteomics analysis was used for the evaluation of the AA-lung injury rats. A total of 6,693 proteins were detected in the lung tissues of AA-lung injury rats using LC-MS/MS and 310 were demonstrated to be DEPs. Among the DEPs, there were a total of 244 proteins upregulated and 66 proteins downregulated in AA-lung injury rats compared with those in CN.

The majority of the top 20 DEPs were related to fatty acid metabolism, immunity, lung inflammation, fibrosis and cancer. For example, arginase 1 competed with eNOS for substrate L-arginine, thereby impairing Enos-dependent NO production, promoting the enzyme to generate reactive oxygen species and finally inducing pulmonary microvascular endothelial cell dysfunction (33). HMGCS2 is a ketogenic rate-limiting enzyme, which is regulated by a variety of transcription

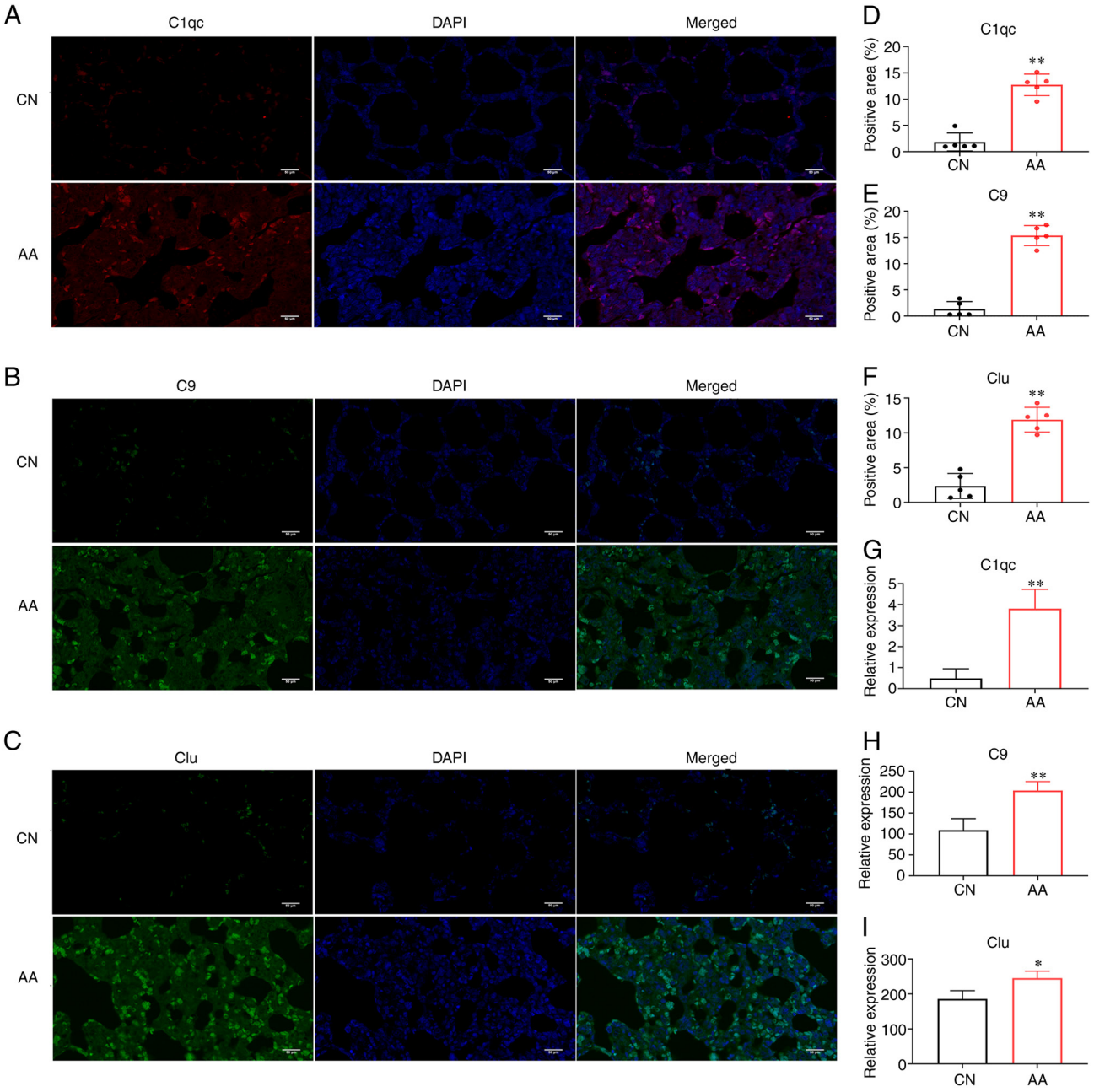

Figure 8. Immunofluorescence results for C1qc, C9 and Clu (x400). (A) Immunofluorescence expression of C1qc. (B) Immunofluorescence expression of C9. (C) Immunofluorescence expression of Clu. Quantitative analysis of immunofluorescence results of (D) C1qc, (E) C9 and (F) Clu proteins. Relative expression of (G) C1qc, (H) C9 and (I) Clu proteins were analyzed by proteomic analysis. *P<0.05 or **P<0.01 vs. CN group in rats. C, complement; CN, control; Clu, clusterin.

factors, including PPAR and Wnt/β-catenin, and it is involved in the pathological process of certain cancers, such as colon cancer and hepatocellular carcinoma (34,35). SLC7A5, an mammalian target of rapamycin complex 1 (mTORC1) activator, is specifically induced by HIF2 α and involved in cancer cell proliferation (36). Recent studies have shown that SLC7A5 is a potential target gene for the interaction between mTORC1 and activating transcription factor 4 signaling, and is associated with airway epithelial cell injury (37). Another study has shown that SLC7A5 is a biomarker of pulmonary fibrosis (38).

In the present study, GO and KEGG enrichment analysis of the DEPs suggested that certain important pathways were associated with lung injury secondary to AA, such as 'fatty acid degradation', 'fatty acid metabolism', 'fatty acid elongation', 'complement and coagulation cascades', 'peroxisome proliferator-activated receptor (PPAR) signaling pathway' and 'hypoxia-inducible factor (HIF)-1 signaling pathway'.

The upregulated DEPs involved in complement and coagulation cascades were C9, C4a, C1qc, Cfb, Cfi, Clu, F12, C4bpa, Serping1 and Itbg2. The complement cascade pathway is an enzymatic cascade reaction, including three activation modes (39): i) The antibody-dependent classical pathway; ii) the non-antibody-dependent bypass pathway; and iii) the mannose-binding lectin pathway. The complement system has a significant function in the immune inflammatory response (40). It can detect and clear pathogens, and also

Table III. Degree (number of links) of differentially expressed proteins of the adjuvant arthritis group in the protein-protein interaction network.

Symbol	Degree	Name	Protein ID	Fold change	P-value	Up/Down regulated
MAPK3	60	Mitogen-activated protein kinase 3	NP_059043.1	0.729	$4.73x10^{-2}$	Down
ITGB1	48	Integrin subunit β 1	NP_058718.2	0.759	$3.77x10^{-2}$	Down
VCL	34	Vinculin	NP_001100718.1	0.818	$5.97x10^{-3}$	Down
APOA4	28	Apolipoprotein A4	NP_036869.1	0.659	$3.15x10^{-2}$	Down
CRYL1	26	Crystallin, lambda 1	NP_786933.1	0.689	$2.74x10^{-2}$	Down
ALDH1A1	22	Aldehyde dehydrogenase 1 family, member A1	NP_071852.2	0.704	$4.05x10^{-2}$	Down
F12	20	Coagulation factor XII	NP_001014028.1	0.668	$4.70x10^{-2}$	Down
MYO1C	16	Myosin 1C	NP_075580.2	0.791	$2.03x10^{-2}$	Down
POLR2E	16	RNA polymerase II, I and III subunit E	XP_006241073.1	0.308	$2.65x10^{-2}$	Down
PSMB5	16	Proteasome 20S subunit β 5	NP_001099197.2	0.797	$2.71x10^{-2}$	Down
EPRS	68	Glutamyl-prolyl-trna synthetase	XP_006250488.1	1.488	$6.50x10^{-3}$	Up
HSPA5	62	Heat shock protein family A (Hsp70) member 5	NP_037215.1	1.313	$1.88x10^{-4}$	Up
GAPDH	58	Glyceraldehyde-3-phosphate dehydrogenase	NP_058704.1	1.295	$4.31x10^{-4}$	Up
EEF2	54	Eukaryotic translation elongation factor 2	NP_058941.1	1.398	$2.49x10^{-2}$	Up
TUFM	54	Tu translation elongation factor, mitochondrial	NP_001099765.1	1.425	$9.82x10^{-3}$	Up
PTPRC	52	Protein tyrosine phosphatase, receptor type, C	NP_001103360.1	2.157	$4.30x10^{-2}$	Up
ITGB2	52	Integrin subunit β 2	NP_001032869.2	2.749	$1.34x10^{-2}$	Up
EEF1G	48	Eukaryotic translationelongation factor 1 gamma	NP_001004223.1	1.355	$3.94x10^{-2}$	Up
HSPA9	48	Hsp70 member 9	NP_001094128.2	1.622	$4.37x10^{-3}$	Up
ACADM	44	Acyl-coa dehydrogenase medium chain	NP_058682.2	1.353	$3.16x10^{-2}$	Up

participates in certain other processes, such as the elimination of immune complexes (40), promoting angiogenesis (41), tissue regeneration (42), fibrosis and lipid metabolism (43). Abnormal activation of the complement system leads to homeostasis imbalance, contributing to a variety of autoimmune and inflammation-related diseases (44). Currently, the role of complement activation in the pathogenesis of lung injury secondary to RA is still unknown, but it may be useful for the development of effective therapies for RA secondary lung injury.

C9 is one of the 11 complement components in blood, which is related to human immunity. C9 often combines with C5b to form a complex in the cell membrane and microorganisms to cause cell lysis. C9 can promote the inflammatory response of lung cells and lung fibrosis (45,46).

The C1q protein, as the first subcomponent of the C1 complex, consists of three polypeptide chains (C1qa, C1qb and C1qc), which can activate the classical complement pathway by binding to a broad range of immune and non-immune ligands. Ogawa *et al* (47) reported that in a silicon-induced pulmonary fibrosis model, the level of C1q increases and presents a pro-fibrotic effect. Alternatively, the increased expression of C1q in bleomycin-induced pulmonary fibrosis in spontaneous pulmonary fibrosis models was considered to be caused by neural precursor cell expressed, developmentally downregulated 4-2 null or mutated surfactant protein C expression in epithelial cells (48).

Clu is a heterodimeric glycoprotein that is widely detected in numerous tissues and fluids, and is regulated by environmental factors. Clu is involved in numerous physiological and pathological processes, such as immune regulation, cell death and cycle regulation, DNA repair, cancer progression (49) and lipid transportation (50) In a long-term hyperoxia-induced lung injury study, a deep relationship between Clu expression and lung injury was found (51). Furthermore, Clu supplementation may alleviate hyperoxia-induced lung cell death (51,52). Zhang *et al* (53) reported that after Clu silencing, the protein

expression levels of a-SMA, collagen I, III and MMP-9 in lung fibroblasts decreased, which inhibited the activation of lung fibroblasts. Besides, inflammatory factors such as IL-6, IL-8 and TNF-α were downregulated in lung fibroblasts to prevent an inflammatory response (53).

C4bp blocks both classical and lectin pathways (54). C4bp acts as a cofactor for factor I, deactivates C3b in the liquid phase, cleaves C4b and accelerates the decay of C3 convertases in classical and lectin pathways (55). C4a is known as an allergenic toxin gene that produces an antimicrobial peptide and a mediator of local inflammation. Previous studies suggested that C4bp and C4a were associated with lung inflammation and injury (56,57).

Cfb, a key alternative pathway gene, has been identified in both RA and interstitial lung disease (58). In addition, previous studies have reported that the downregulating methylation of Cfb is associated with lung inflammation caused by the activation of pulmonary macrophages (59,60). Another study reported that Cfb was associated with pulmonary airway inflammation in a mouse model of collagen-induced arthritis lung disease (61).

SERPING1, also known as C1 inhibitor, is one of the complement regulatory factors, which can regulate the activation, persistence and function of complement by inhibiting complement protease or competitively binding with pattern recognition molecules and complement invertase (62). SERPING1is highly expressed in the lung tissue of mice (63) and is also expressed in 70% of mesothelial cells (64) and fibroblasts (65,66).

It can be concluded that the DEPs related to complement and coagulation cascades serve an important role in the process of lung inflammation, immunity and fibrosis. Therefore, these DEPs can act as a reference in experiments to identify potential biomarkers for early diagnosis and the prevention of RA lung injury. Furthermore, the aforementioned studies have shown that immune responses, especially complement cascades, are involved in certain types of lung injury (67). For this reason, C1qc, Clu and C9 were selected for validation by immunofluorescence assay and their expression in the lung tissues of the AA-lung injury group was found to be significantly upregulated compared with that in the CN group, consistent with the results from proteomics analysis. Although these complement genes were found to be upregulated in RA or lung diseases, their role in RA-lung injury still needs to be further explored.

In recent years, studies on fatty acid metabolism have been reported. A number of studies have reported that fatty acid metabolism-related genes are involved in lung inflammation (68), immune homeostasis (69,70), apoptosis (71), lung fibrosis (72) and other processes. In the present study, it was demonstrated that the upregulated DEPs associated with fatty acid metabolism included ERLIN1, ACADL, ACADM and ACOX1. ERLIN1 is a gene that encodes ER inhibin (73) and cholesterol regulator (74) and serves an important role in immune cell metabolism (75). In a cross-disease meta-analysis, ERLIN1 has been reported to be a regulatory site in common between psoriasis and type 2 diabetes, and its resulting protein was linked by the NF-κB pathway (75). ACADL and ACADM are the first steps to catalyze the oxidation of serum-free fatty acids, while ACOX1 is key in the oxidation of serum-free fatty acids in peroxisomes (76,77). ACOX1 is located downstream of the PPARα signaling pathway and serves as a pivotal role in the rate-limiting enzyme in fatty acid β oxidation (78). The overexpression of ACOX1 promotes the synthesis and release of inflammatory factors such as TNF-α (79). At present, the genes related to lipid metabolism, such as ERLIN1, ACADL, ACADM and ACOX1, lack research in RA-lung disease. Therefore, it was hypothesized that these genes might be related to the abnormal function of lung cells caused by the disturbance of immune cell metabolism.

PPAR-γ is a nuclear transcription receptor that has effects in anti-inflammatory and cytoprotective. PPAR-γ can promote the expression of PTEN and inhibits the TGF-β1, PI3K/Akt and SMAD signaling pathways, whilst it can activate the SMAD7- signaling pathway to inhibit lung fibrosis (80,81).

HIF-1α is a transcription activator, which serves an important role in numerous pathological processes, such as rheumatoid arthritis (82), systemic lupus erythematosus (83) and inflammatory bowel disease (84). HIF-1α has been confirmed to be involved in the pathogenesis of chronic obstructive pulmonary disease (COPD) by regulating VEGF upregulation (85). Moreover, the HIF-1α signaling pathway as been reported to be activated in smokers with COPD (86). Overexpression of HIF-1α-related proteins is associated with a decrease in lung function and fibrosis (87,88).

In summary, in the present study the protein expression profiles of lung tissues were compared between AA-lung injury and normal mice. Based on the GO and KEGG analysis, the potential mechanism and biomarkers of RA-lung injury were highlighted. Furthermore, complement and coagulation cascades as well as fatty acid metabolism pathways were demonstrated to be related to lung injury in AA.

Nevertheless, the present study had several limitations: i) The specific molecular mechanism of how these DEPs regulates RA lung injury is still unclear and the studies on this are still at an early stage; ii) modeling the full complexity of human disease in animals is difficult and is not sufficient to elucidate the biological mechanisms of lung injury in patients with rheumatoid arthritis; iii) there were only six rats in each group for the animal experiments in the present study, and the lack of cell trials and clinical samples for the study may affect the results of the present study; iv) in-depth experimental studies to clarify the exact molecular mechanism of RA lung injury are still needed in the future.

Acknowledgements

Not applicable.

Funding

The present study was supported by the National Natural Science Foundation of China (grant nos. 82004102, 82174211 and 81804051), the Project Funded by China Postdoctoral Science Foundation (grant no. 2022M721533) and the Science and Technology Program of Guangzhou, China (grant no. 2023A04J2481).

Availability of data and materials

The datasets generated and/or analyzed during the current study are available in the iProX repository, https://www.iprox.

cn/page/ProjectFileList.html?projectId=IPX0006495000&url=1686278190812oyzK, data set identifier IPX0006495000. Any remaining datasets used and/or analyzed during the current study are available from the corresponding author on reasonable request.

Authors' contributions

PHZ, CHX and JL conceived the study and designed the present study. PHZ, ESC, DBW and JTW performed the experiments and collected the data. PHZ and CHX analysed the data and confirm the authenticity of all the raw data. PHZ was a major contributor in writing the manuscript. CHX revised the study critically for important intellectual content. All authors have read and approved the final manuscript.

Ethics approval and consent to participate

The animal study was approved by the Animal Ethics Committee of Anhui University of Traditional Chinese Medicine (approval no. 2021022) and complied with the Guide of the Health Care and Use of Laboratory Animals.

Patient consent for publication

Not applicable.

Competing interests

The authors declare that they have no competing interests.

References

1. Prasad P, Verma S, Surbhi, Ganguly NK, Chaturvedi V and Mittal SA: Rheumatoid arthritis: Advances in treatment strategies. Mol Cell Biochem 478: 69-88, 2023.
2. Kan S, Duan M, Liu Y, Wang C and Xie J: Role of mitochondria in physiology of chondrocytes and diseases of osteoarthritis and rheumatoid arthritis. Cartilage 13 (2 Suppl): 1102S-1121S, 2021.
3. Zhou S and Huang G: Some important inhibitors and mechanisms of rheumatoid arthritis. Chem Biol Drug Des 99: 930-943, 2022.
4. Minichiello E, Semerano L and Boissier MC: Time trends in the incidence, prevalence, and severity of rheumatoid arthritis: A systematic literature review. Joint Bone Spine 83: 625-630, 2016.
5. Akiyama M and Kaneko Y: Pathogenesis, clinical features, and treatment strategy for rheumatoid arthritis-associated interstitial lung disease. Autoimmun Rev 21: 103056, 2022.
6. Kelly C, Emery P and Dieudé P: Current issues in rheumatoid arthritis-associated interstitial lung disease. Lancet Rheumatol 3: e798-e807, 2021.
7. Conforti A, Di Cola I, Pavlych V, Ruscitti P, Berardicurti O, Ursini F, Giacomelli R and Cipriani P: Beyond the joints, the extra-articular manifestations in rheumatoid arthritis. Autoimmun Rev 20: 102735, 2021.
8. Akira M, Sakatani M and Hara H: Thin-section CT findings in rheumatoid arthritis-associated lung disease: CT patterns and their courses. J Comput Assist Tomogr 23: 941-948, 1999.
9. Koduri G, Norton S, Young A, Cox N, Davies P, Devlin J, Dixey J, Gough A, Prouse P, Winfield J, *et al*: Interstitial lung disease has a poor prognosis in rheumatoid arthritis: Results from an inception cohort. Rheumatology (Oxford) 49: 1483-1489, 2010.
10. Lee HK, Kim DS, Yoo B, Seo JB, Rho JY, Colby TV and Kitaichi M: Histopathologic pattern and clinical features of rheumatoid arthritis-associated interstitial lung disease. Chest 127: 2019-2027, 2005.
11. Zamora-Legoff JA, Krause ML, Crowson CS, Ryu JH and Matteson EL: Progressive decline of lung function in rheumatoid arthritis-associated interstitial lung disease. Arthritis Rheumatol 69: 542-549, 2017.
12. Vergnenègre A, Pugnere N, Antonini MT, Arnaud M, Melloni B, Treves R and Bonnaud F: Airway obstruction and rheumatoid arthritis. Eur Respir J 10: 1072-1078, 1997.
13. Bilgici A, Ulusoy H, Kuru O, Celenk C, Unsal M and Danacı M: Pulmonary involvement in rheumatoid arthritis. Rheumatol Int 25: 429-435, 2005.
14. Natalini JG, Swigris JJ, Morisset J, Elicker BM, Jones KD, Fischer A, Collard HR and Lee JS: Understanding the determinants of health-related quality of life in rheumatoid arthritis-associated interstitial lung disease. Respir Med 127: 1-6, 2017.
15. Singh N, Varghese J, England BR, Solomon JJ, Michaud K, Mikuls TR, Healy HS, Kimpston EM and Schweizer ML: Impact of the pattern of interstitial lung disease on mortality in rheumatoid arthritis: A systematic literature review and meta-analysis. Semin Arthritis Rheum 49: 358-365, 2019.
16. Shaw M, Collins BF, Ho LA and Raghu G: Rheumatoid arthritis-associated lung disease. Eur Respir Rev 24: 1-16, 2015.
17. Aslam B, Basit M, Nisar MA, Khurshid M and Rasool MH: Proteomics: Technologies and their applications. J Chromatogr Sci 55: 182-196, 2017.
18. Yasuda T, Tahara K and Sawada T: Detection of salivary citrullinated cytokeratin 13 in healthy individuals and patients with rheumatoid arthritis by proteomics analysis. PLoS One 17: e0265687, 2022.
19. Liu S, Ji W, Lu J, Tang X, Guo Y, Ji M, Xu T, Gu W, Kong D, Shen Q, *et al*: Discovery of potential serum protein biomarkers in ankylosing spondylitis using tandem mass tag-based quantitative proteomics. J Proteome Res 19: 864-872, 2020.
20. Zhou G, Wei P, Lan J, He Q, Guo F, Guo Y, Gu W, Xu T and Liu S: TMT-based quantitative proteomics analysis and potential serum protein biomarkers for systemic lupus erythematosus. Clin Chim Acta 534: 43-49, 2022.
21. Wu X, Jeong Y, Poli de Frías S, Easthausen I, Hoffman K, Oromendia C, Taheri S, Esposito AJ, Quesada Arias L, Ayaub EA, *et al*: Serum proteomic profiling of rheumatoid arthritis-interstitial lung disease with a comparison to idiopathic pulmonary fibrosis. Thorax 77: 1041-1044, 2022.
22. Song LN, Kong XD, Wang HJ and Zhan LB: Establishment of a rat adjuvant arthritis-interstitial lung disease model. Biomed Res Int 2016: 2970783, 2016.
23. National Institutes of Health (U.S.). Office for Protection from Research Risks: Public Health Service policy on humane care and use of laboratory animals. Office for Protection from Research Risks (OPRR), National Institutes of Health, 1986.
24. An ZP: BS: Lung function test in wistar rats. Chin J Lab Anim Sci 12: 102-104, 2013.
25. Wei X, Zhou R, Chen Y, Ma G, Yang Y, Lu C, Xu W and Hu W: Systemic pharmacological verification of Baixianfeng decoction regulating TNF-PI3K-Akt-NF-κB pathway in treating rheumatoid arthritis. Bioorg Chem 119: 105519, 2022.
26. Goldner J: A modification of the masson trichrome technique for routine laboratory purposes. Am J Pathol 14: 237-243, 1938.
27. Szapiel SV, Elson NA, Fulmer JD, Hunninghake GW and Crystal RG: Bleomycin-induced interstitial pulmonary disease in the nude, athymic mouse. Am Rev Respir Dis 120: 893-899, 1979.
28. Wiśniewski JR, Zougman A, Nagaraj N and Mann M: Universal sample preparation method for proteome analysis. Nat Methods 6: 359-362, 2009.
29. Chen C, Chen H, Zhang Y, Thomas HR, Frank MH, He Y and Xia R: TBtools: An integrative toolkit developed for interactive analyses of big biological data. Mol Plant 13: 1194-1202, 2020.
30. Figus FA, Piga M, Azzolin I, McConnell R and Iagnocco A: Rheumatoid arthritis: Extra-articular manifestations and comorbidities. Autoimmun Rev 20: 102776, 2021.
31. Schurgers E, Mertens F, Vanoirbeek JA, Put S, Mitera T, De Langhe E, Billiau A, Hoet PH, Nemery B, Verbeken E and Matthys P: Pulmonary inflammation in mice with collagen-induced arthritis is conditioned by complete Freund's adjuvant and regulated by endogenous IFN-γ. Eur J Immunol 42: 3223-3234, 2012.
32. Lei W and Jian L: Changes of CD4(+) CD25(+) regulatory T cells, FoxP3 in adjuvant arthritis rats with damage of pulmonary function and effects of tripterygium glycosides tablet. Int J Rheumatol 2012: 348450, 2012.

33. Lucas R, Czikora I, Sridhar S, Zemskov EA, Oseghale A, Circo S, Cederbaum SD, Chakraborty T, Fulton DJ, Caldwell RW and Romero MJ: Arginase 1: An unexpected mediator of pulmonary capillary barrier dysfunction in models of acute lung injury. Front Immunol 4: 228, 2013.
34. Kim JT, Li C, Weiss HL, Zhou Y, Liu C, Wang Q and Evers BM: Regulation of ketogenic enzyme HMGCS2 by Wnt/β-catenin/PPARγ pathway in intestinal cells. Cells 8: 1106, 2019.
35. Su SG, Yang M, Zhang MF, Peng QZ, Li MY, Liu LP and Bao SY: miR-107-mediated decrease of HMGCS2 indicates poor outcomes and promotes cell migration in hepatocellular carcinoma. Int J Biochem Cell Biol 91: 53-59, 2017.
36. Elorza A, Soro-Arnáiz I, Meléndez-Rodríguez F, Rodríguez-Vaello V, Marsboom G, de Cárcer G, Acosta-Iborra B, Albacete-Albacete L, Ordóñez A, Serrano-Oviedo L, *et al*: HIF2α acts as an mTORC1 activator through the amino acid carrier SLC7A5. Mol Cell 48: 681-691, 2012.
37. Sokolov AM, Holmberg JC and Feliciano DM: The amino acid transporter Slc7a5 regulates the mTOR pathway and is required for granule cell development. Hum Mol Genet 29: 3003-3013, 2020.
38. Nojima Y, Takeda Y, Maeda Y, Bamba T, Fukusaki E, Itoh MN, Mizuguchi K and Kumanogoh A: Metabolomic analysis of fibrotic mice combined with public RNA-Seq human lung data reveal potential diagnostic biomarker candidates for lung fibrosis. FEBS Open Bio 10: 2427-2436, 2020.
39. Ehrnthaller C, Ignatius A, Gebhard F and Huber-Lang M: New insights of an old defense system: Structure, function, and clinical relevance of the complement system. Mol Med 17: 317-329, 2011.
40. Dunkelberger JR and Song WC: Complement and its role in innate and adaptive immune responses. Cell Res 20: 34-50, 2010.
41. Hanna J, Ah-Pine F, Boina C, Bedoui Y, Gasque P and Septembre-Malaterre A: Deciphering the role of the anaphylatoxin C3a: A key function in modulating the tumor microenvironment. Cancers (Basel) 15: 2986, 2023.
42. Monk PN, Scola AM, Madala P and Fairlie DP: Function, structure and therapeutic potential of complement C5a receptors. Br J Pharmacol 152: 429-448, 2007.
43. Guo Z, Fan X, Yao J, Tomlinson S, Yuan G and He S: The role of complement in nonalcoholic fatty liver disease. Front Immunol 13: 1017467, 2022.
44. Triggianese P, Conigliaro P, De Martino E, Monosi B and Chimenti MS: Overview on the link between the complement system and auto-immune articular and pulmonary disease. Open Access Rheumatol 15: 65-79, 2023.
45. Luo R, Wang T, Zhuo S, Guo X and Ma D: Excessive hydrogen sulfide causes lung and brain tissue damage by promoting PARP1/Bax and C9 and inhibiting LAMB1. Apoptosis 27: 149-160, 2022.
46. Pellicano C, Miglionico M, Romaggioli L, Colalillo A, Vantaggio L, Napodano C, Callà C, Gulli F, Marino M, Basile U and Rosato E: Increased Complement activation in systemic sclerosis patients with skin and lung fibrosis. J Pers Med 12: 284, 2022.
47. Ogawa T, Shichino S, Ueha S, Ogawa S and Matsushima K: Complement protein C1q activates lung fibroblasts and exacerbates silica-induced pulmonary fibrosis in mice. Biochem Biophys Res Commun 603: 88-93, 2022.
48. Duerr J, Leitz DHW, Szczygiel M, Dvornikov D, Fraumann SG, Kreutz C, Zadora PK, Seyhan Agircan A, Konietzke P, Engelmann TA, *et al*: Conditional deletion of Nedd4-2 in lung epithelial cells causes progressive pulmonary fibrosis in adult mice. Nat Commun 11: 2012, 2020.
49. Zhang Y, Lv X, Chen L and Liu Y: The role and function of CLU in cancer biology and therapy. Clin Exp Med: Sep 13, 2022 (Epub ahead of print).
50. Ishikawa Y, Ishii T, Akasaka Y, Masuda T, Strong JP, Zieske AW, Takei H, Malcom GT, Taniyama M, Choi-Miura NH and Tomita M: Immunolocalization of apolipoproteins in aortic atherosclerosis in American youths and young adults: Findings from the PDAY study. Atherosclerosis 158: 215-225, 2001.
51. Hong JY, Kim MN, Kim EG, Lee JW, Kim HR, Kim SY, Lee SM, Kim YH, Kim KW and Sohn MH: Clusterin deficiency exacerbates hyperoxia-induced acute lung injury. Cells 10: 944, 2021.
52. Fox CR and Parks GD: Complement inhibitors vitronectin and clusterin are recruited from human serum to the surface of coronavirus OC43-infected lung cells through antibody-dependent mechanisms. Viruses 14: 29, 2021.
53. Zhang Q, Yue Y and Zheng R: Clusterin as a serum biomarker candidate contributes to the lung fibroblasts activation in chronic obstructive pulmonary disease. Chin Med J (Engl) 135: 1076-1086, 2022.
54. Blom AM, Kask L and Dahlbäck B: Structural requirements for the complement regulatory activities of C4BP. J Biol Chem 276: 27136-27144, 2001.
55. Ermert D and Blom AM: C4b-binding protein: The good, the bad and the deadly. Novel functions of an old friend. Immunol Lett 169: 82-92, 2016.
56. Khadzhieva M, Kuzovlev AN and Salnikova LE: Pneumonia: Host susceptibility and shared genetics with pulmonary function and other traits. Clin Exp Immunol 198: 367-380, 2019.
57. Dasari P, Koleci N, Shopova IA, Wartenberg D, Beyersdorf N, Dietrich S, Sahagún-Ruiz A, Figge MT, Skerka C, Brakhage AA and Zipfel PF: Enolase from Aspergillus fumigatus is a moonlighting protein that binds the human plasma complement proteins factor H, FHL-1, C4BP, and plasminogen. Front Immunol 10: 2573, 2019.
58. Kulkarni HS, Liszewski MK, Brody SL and Atkinson JP: The complement system in the airway epithelium: An overlooked host defense mechanism and therapeutic target? J Allergy Clin Immunol 141: 1582-1586 e1, 2018.
59. Kyung Lee M, Armstrong DA, Hazlett HF, Dessaint JA, Mellinger DL, Aridgides DS, Christensen BC and Ashare A: Exposure to extracellular vesicles from Pseudomonas aeruginosa result in loss of DNA methylation at enhancer and DNase hypersensitive site regions in lung macrophages. Epigenetics 16: 1187-1200, 2021.
60. Armstrong DA, Lee MK, Hazlett HF, Dessaint JA, Mellinger DL, Aridgides DS, Hendricks GM, Abdalla MAK, Christensen BC and Ashare A: Extracellular vesicles from Pseudomonas aeruginosa suppress MHC-related molecules in human lung macrophages. Immunohorizons 4: 508-519, 2020.
61. Gaurav R, Mikuls TR, Thiele GM, Nelson AJ, Niu M, Guda C, Eudy JD, Barry AE, Wyatt TA, Romberger DJ, *et al*: High-throughput analysis of lung immune cells in a combined murine model of agriculture dust-triggered airway inflammation with rheumatoid arthritis. PLoS One 16: e0240707, 2021.
62. Ricklin D, Hajishengallis G, Yang K and Lambris JD: Complement: A key system for immune surveillance and homeostasis. Nat Immunol 11: 785-797, 2010.
63. Lener M, Vinci G, Duponchel C, Meo T and Tosi M: Molecular cloning, gene structure and expression profile of mouse C1 inhibitor. Eur J Biochem 254: 117-122, 1998.
64. Chaudhary N, Jayaraman A, Reinhardt C, Campbell JD and Bosmann M: A single-cell lung atlas of complement genes identifies the mesothelium and epithelium as prominent sources of extrahepatic complement proteins. Mucosal Immunol 15: 927-939, 2022.
65. Danobeitia JS, Ziemelis M, Ma X, Zitur LJ, Zens T, Chlebeck PJ, Van Amersfoort ES and Fernandez LA: Complement inhibition attenuates acute kidney injury after ischemia-reperfusion and limits progression to renal fibrosis in mice. PLoS One 12: e0183701, 2017.
66. Curci C, Castellano G, Stasi A, Divella C, Loverre A, Gigante M, Simone S, Cariello M, Montinaro V, Lucarelli G, *et al*: Endothelial-to-mesenchymal transition and renal fibrosis in ischaemia/reperfusion injury are mediated by complement anaphylatoxins and Akt pathway. Nephrol Dial Transplant 29: 799-808, 2014.
67. Yang Z, Nicholson SE, Cancio TS, Cancio LC and Li Y: Complement as a vital nexus of the pathobiological connectome for acute respiratory distress syndrome: An emerging therapeutic target. Front Immunol 14: 1100461, 2023.
68. Kotlyarov S and Kotlyarova A: Anti-Inflammatory function of fatty acids and involvement of their metabolites in the resolution of inflammation in chronic obstructive pulmonary disease. Int J Mol Sci 22: 12803, 2021.
69. Kočar E, Režen T and Rozman D: Cholesterol, lipoproteins, and COVID-19: Basic concepts and clinical applications. Biochim Biophys Acta Mol Cell Biol Lipids 1866: 158849, 2021.
70. Tanner JE and Alfieri C: The fatty acid lipid metabolism nexus in COVID-19. Viruses 13: 90, 2021.
71. Hu X, Ge X, Liang W, Shao Y, Jing J, Wang C, Zeng R and Yao B: Effects of saturated palmitic acid and omega-3 polyunsaturated fatty acids on Sertoli cell apoptosis. Syst Biol Reprod Med 64: 368-380, 2018.

72. Chu SG, Villalba JA, Liang X, Xiong K, Tsoyi K, Ith B, Ayaub EA, Tatituri RV, Byers DE, Hsu FF, *et al*: Palmitic acid-rich high-fat diet exacerbates experimental pulmonary fibrosis by modulating endoplasmic reticulum stress. Am J Respir Cell Mol Biol 61: 737-746, 2019.
73. Jo Y, Sguigna PV and DeBose-Boyd RA: Membrane-associated ubiquitin ligase complex containing gp78 mediates sterol-accelerated degradation of 3-hydroxy-3-methylglutaryl-coenzyme A reductase. J Biol Chem 286: 15022-15031, 2011.
74. Huang SSY, Toufiq M, Saraiva LR, Van Panhuys N, Chaussabel D and Garand M: Transcriptome and literature mining highlight the differential expression of ERLIN1 in immune cells during sepsis. Biology (Basel) 10: 755, 2021.
75. Patrick MT, Stuart PE, Zhang H, Zhao Q, Yin X, He K, Zhou XJ, Mehta NN, Voorhees JJ, Boehnke M, *et al*: Causal relationship and shared genetic loci between psoriasis and type 2 diabetes through trans-disease meta-analysis. J Invest Dermatol 141: 1493-1502, 2021.
76. Ma APY, Yeung CLS, Tey SK, Mao X, Wong SWK, Ng TH, Ko FCF, Kwong EML, Tang AHN, Ng IO, *et al*: Suppression of ACADM-mediated fatty acid oxidation promotes hepatocellular carcinoma via aberrant CAV1/SREBP1 signaling. Cancer Res 81: 3679-3692, 2021.
77. Dong Y, Lu H, Li Q, Qi X, Li Y, Zhang Z, Chen J and Ren J: (5R)-5-hydroxytriptolide ameliorates liver lipid accumulation by suppressing lipid synthesis and promoting lipid oxidation in mice. Life Sci 232: 116644, 2019.
78. Xu Y, Denning KL and Lu Y: PPARα agonist WY-14,643 induces the PLA2/COX-2/ACOX1 pathway to enhance peroxisomal lipid metabolism and ameliorate alcoholic fatty liver in mice. Biochem Biophys Res Commun 613: 47-52, 2022.
79. Kong A, Xu D, Hao T, Liu Q, Zhan R, Mai K and Ai Q: Role of acyl-coenzyme A oxidase 1 (ACOX1) on palmitate-induced inflammation and ROS production of macrophages in large yellow croaker (Larimichthys crocea). Dev Comp Immunol 136: 104501, 2022.
80. Vallée A, Lecarpentier Y, Guillevin R and Vallée JN: Interactions between TGF-β1, canonical WNT/β-catenin pathway and PPAR γ in radiation-induced fibrosis. Oncotarget 8: 90579-90604, 2017.
81. Milam JE, Keshamouni VG, Phan SH, Hu B, Gangireddy SR, Hogaboam CM, Standiford TJ, Thannickal VJ and Reddy RC: PPAR-gamma agonists inhibit profibrotic phenotypes in human lung fibroblasts and bleomycin-induced pulmonary fibrosis. Am J Physiol Lung Cell Mol Physiol 294: L891-L901, 2008.
82. Biniecka M, Canavan M, McGarry T, Gao W, McCormick J, Cregan S, Gallagher L, Smith T, Phelan JJ, Ryan J, *et al*: Dysregulated bioenergetics: A key regulator of joint inflammation. Ann Rheum Dis 75: 2192-2200, 2016.
83. Ma C, Wei J, Zhan F, Wang R, Fu K, Wan X and Li Z: Urinary hypoxia-inducible factor-1alpha levels are associated with histologic chronicity changes and renal function in patients with lupus nephritis. Yonsei Med J 53: 587-592, 2012.
84. Manresa MC and Taylor CT: Hypoxia inducible factor (HIF) hydroxylases as regulators of intestinal epithelial barrier function. Cell Mol Gastroenterol Hepatol 3: 303-315, 2017.
85. Fu X and Zhang F: Role of the HIF-1 signaling pathway in chronic obstructive pulmonary disease. Exp Ther Med 16: 4553-4561, 2018.
86. Yu H, Li Q, Kolosov VP, Perelman JM and Zhou X: Regulation of cigarette smoke-mediated mucin expression by hypoxia-inducible factor-1α via epidermal growth factor receptor-mediated signaling pathways. J Appl Toxicol 32: 282-292, 2012.
87. Tzouvelekis A, Harokopos V, Paparountas T, Oikonomou N, Chatziioannou A, Vilaras G, Tsiambas E, Karameris A, Bouros D and Aidinis V: Comparative expression profiling in pulmonary fibrosis suggests a role of hypoxia-inducible factor-1alpha in disease pathogenesis. Am J Respir Crit Care Med 176: 1108-1119, 2007.
88. Bryant AJ, Carrick RP, McConaha ME, Jones BR, Shay SD, Moore CS, Blackwell TR, Gladson S, Penner NL, Burman A, *et al*: Endothelial HIF signaling regulates pulmonary fibrosis-associated pulmonary hypertension. Am J Physiol Lung Cell Mol Physiol 310: L249-L262, 2016.